Electronic Supplementary Material (ESI) for New Journal of Chemistry.
This journal is © The Royal Society of Chemistry and the Centre National de la Recherche Scientifique 2022

Two-dimensional type-II $XSi_2P_4/MoTe_2$ (X=Mo, W) van der Waals heterostructures with tunable electronic and optical properties

Qingqing Luo[a], Shaoqian Yin[a,*], Xiaoxin Sun[a], Yanan Tang[b], Zhen Feng[c], and Xianqi Dai[a,*]

[a] School of Physics, Henan Normal University, Xinxiang, Henan 453007, China.

[b] School of Physics and Electronic Engineering, Zhengzhou Normal University, Zhengzhou, Henan 450044, China.

[c] School of Materials Science and Engineering, Henan Engineering Research Center for Modification Technology of Metal Materials, Henan Institute of Technology, Xinxiang, Henan 453000, China

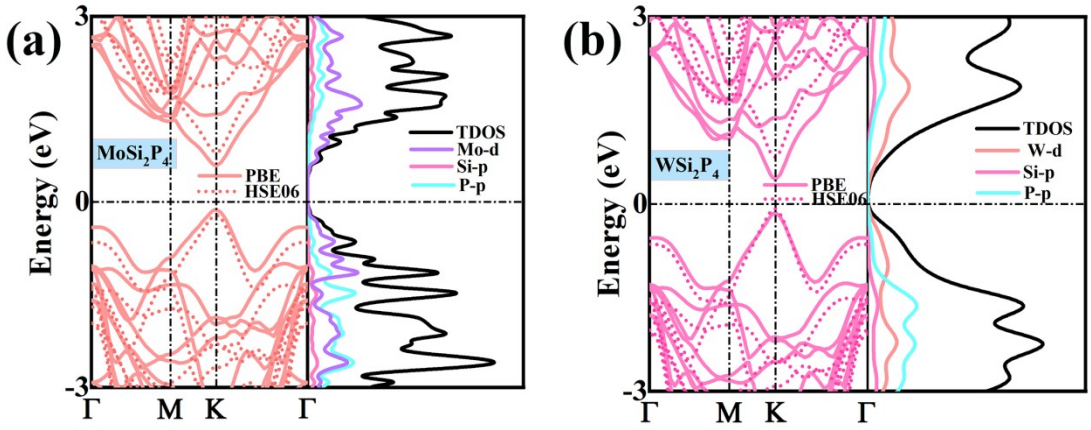

Fig. S1. The band structures and corresponding PDOS for $MoSi_2P_4$ and WSi_2P_4 monolayers

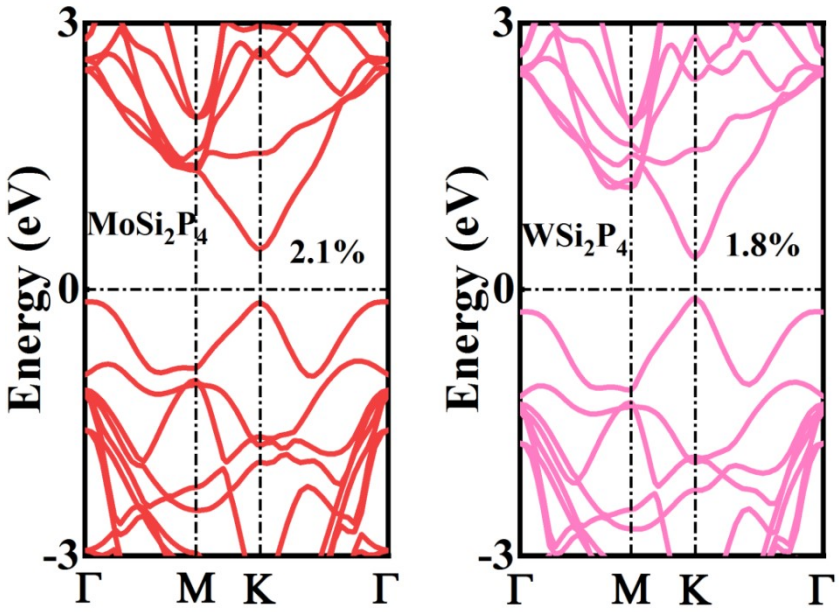

Fig. S2. Calculated the band structures of $MoSi_2P_4/WSi_2P_4$ under tensile 2.1% /1.8%

* Address correspondence to E-mail:ysq@htu.edu.cn (Shaoqian Yin), xqdai@htu.edu.cn (Xianqi Dai)

Table S1

Calculated the binding energy E_b (eV) and cohesive energy E_{coh} (eV) of different models for the $MoSi_2P_4/MoTe_2$ and $WSi_2P_4/MoTe_2$ heterostructures

	A1	A2	A3	A4	A5
E_b (eV)	-0.254	-0.241	-0.177	-0.173	-0.270
E_{coh} (eV)	-5.512	-5.511	-5.504	-5.504	-5.514
	B1	B2	B3	B4	B5
E_b (eV)	-0.298	-0.218	-0.218	-0.220	-0.361
E_{coh} (eV)	-4.766	-4.758	-4.758	-4.756	-4.767

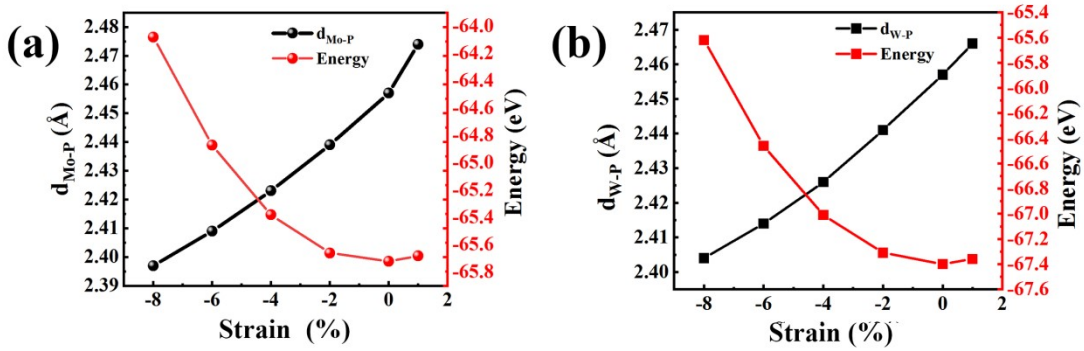

Fig. S3. The bond lengths (d_{Mo-P} and d_{W-P}) and total energies under different strains for the (a) $MoSi_2P_4/WSi_2P_4$ and (b) WSi_2P_4/WSi_2P_4 heterostructures.

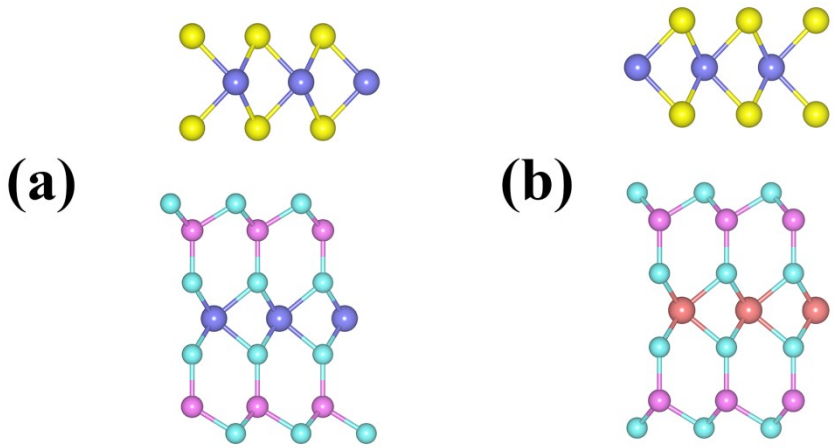

Fig. S4. The optimized structures of (a) $MoSi_2P_4/MoTe_2$ heterostructure and (b) $WSi_2P_4/MoTe_2$ heterostructure under biaxial strain ε=-9%. (Where the purple, watermelon red, pink, cyan and yellow spheres represent the Mo, W, Si, P and Se elements, respectively).

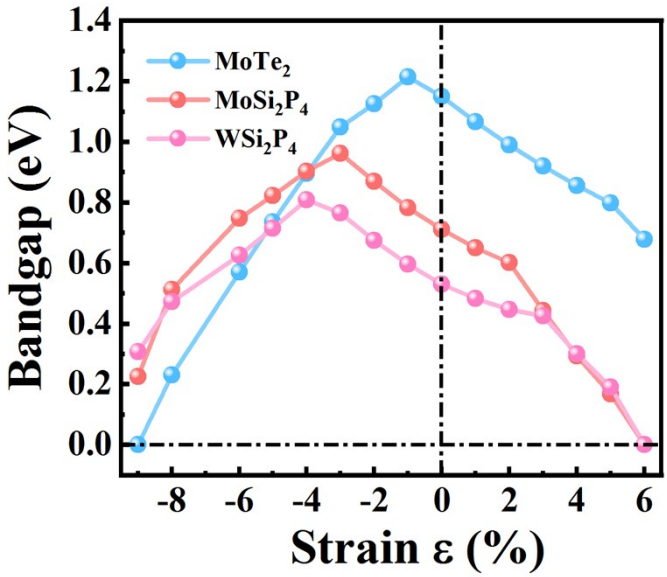

Fig. S5. The bandgap as of $MoSi_2P_4$, WSi_2P_4 and $MoTe_2$ as functions with various biaxial strains

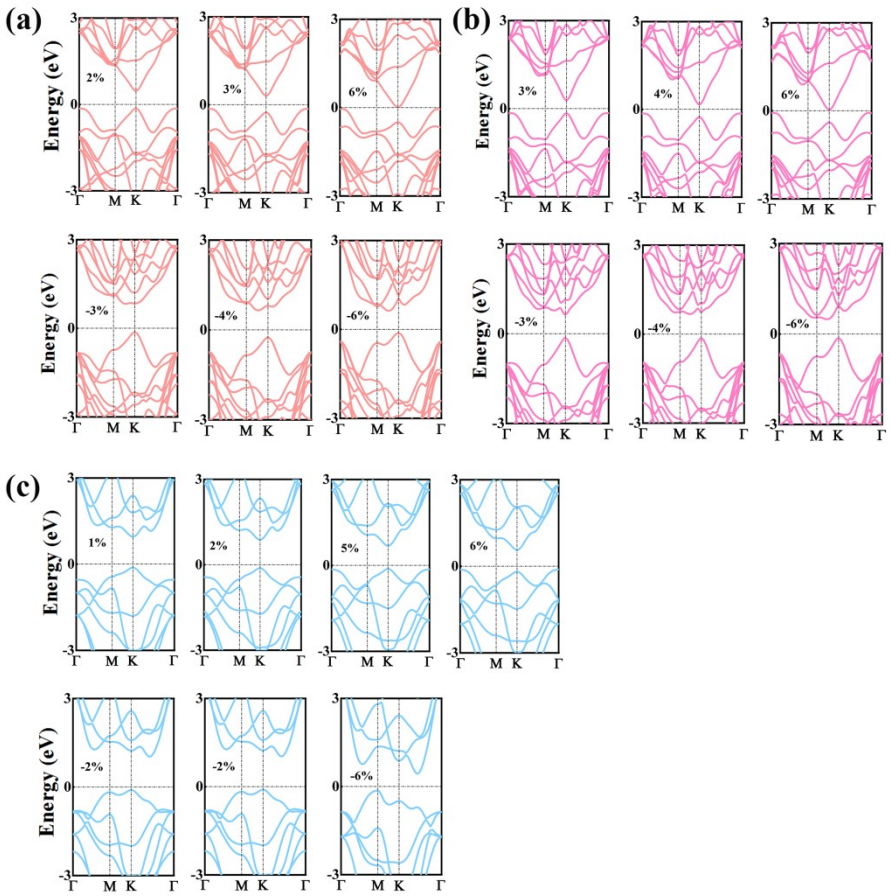

Fig. S6. The band structures of (a) $MoSi_2P_4$, (b) WSi_2P_4 and (c) MoTe2 under different strains

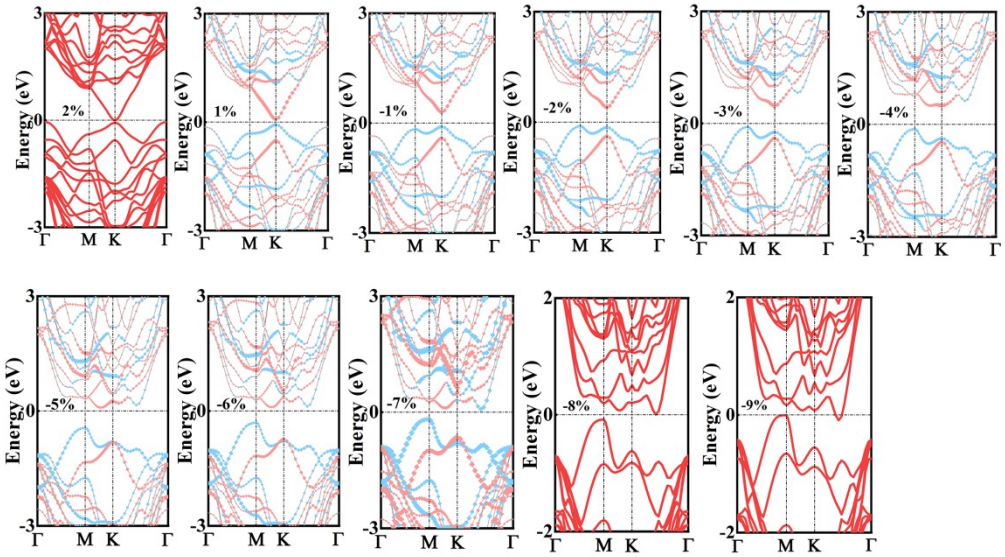

Fig. S7. The projected band structures of the $MoSi_2P_4/MoTe_2$ vdWHs under different biaxial strains

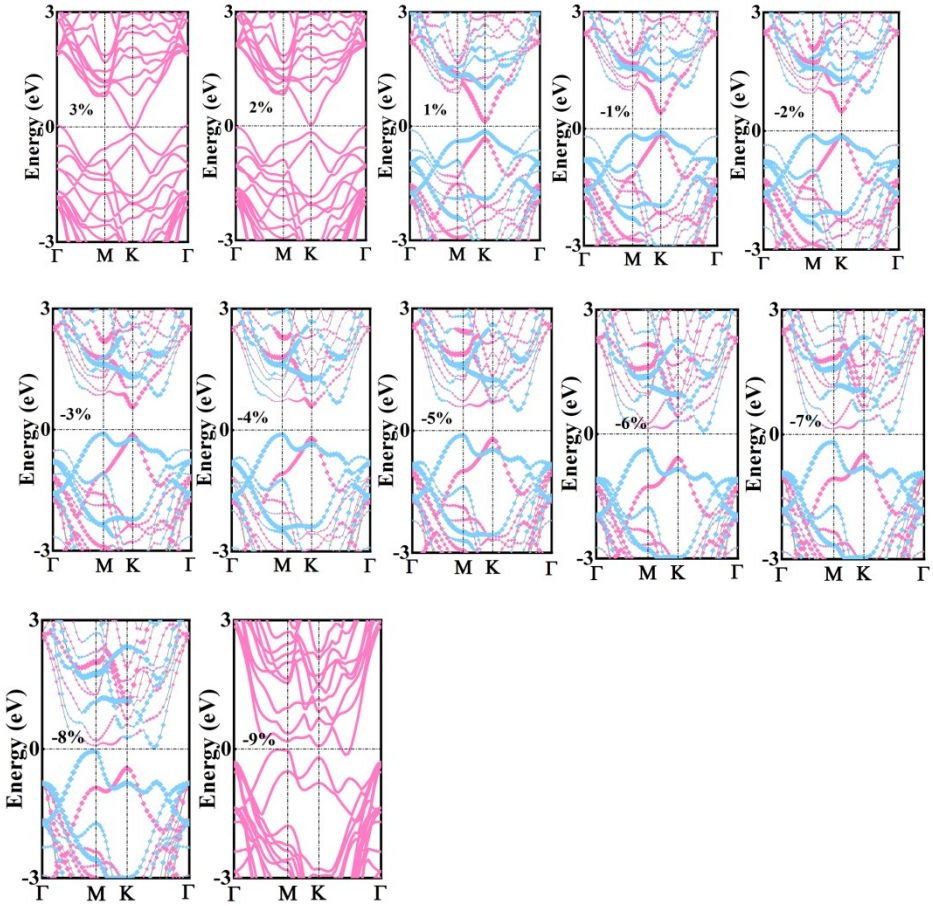

Fig. S8. The projected band structures of the $WSi_2P_4/MoTe_2$ vdWHs under different biaxial strains

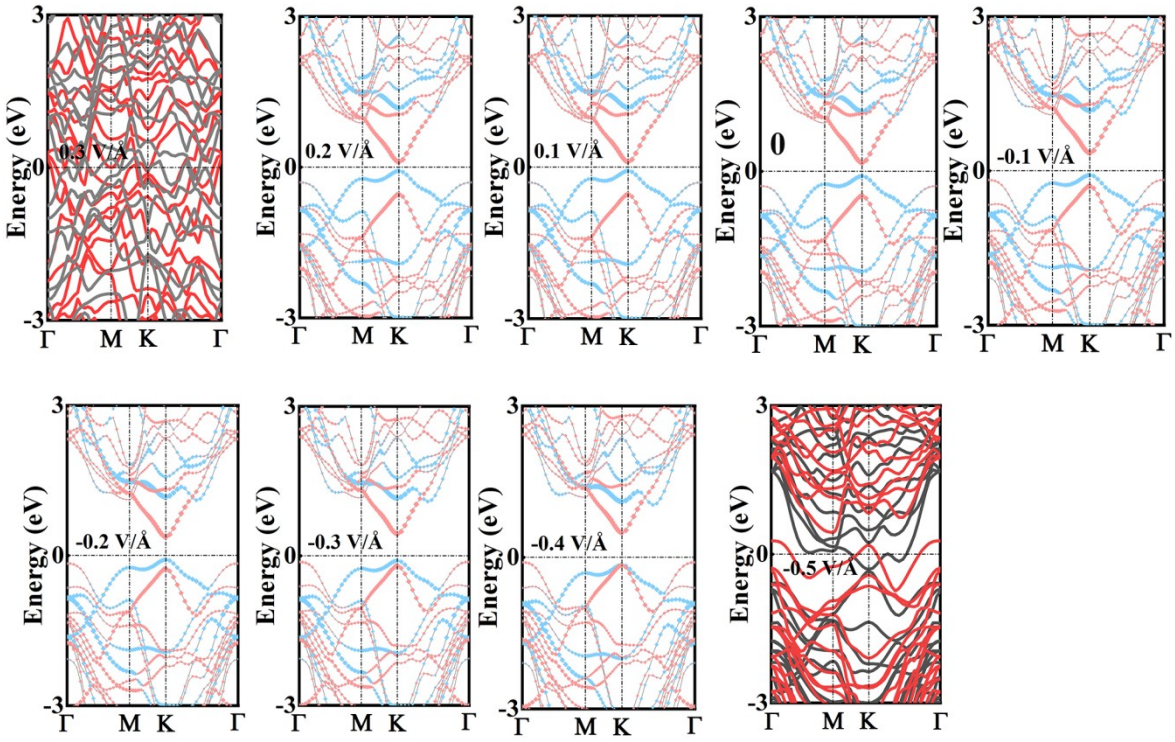

Fig. S9. The projected band structures of the $MoSi_2P_4/MoTe_2$ vdWHs under different external electric fields

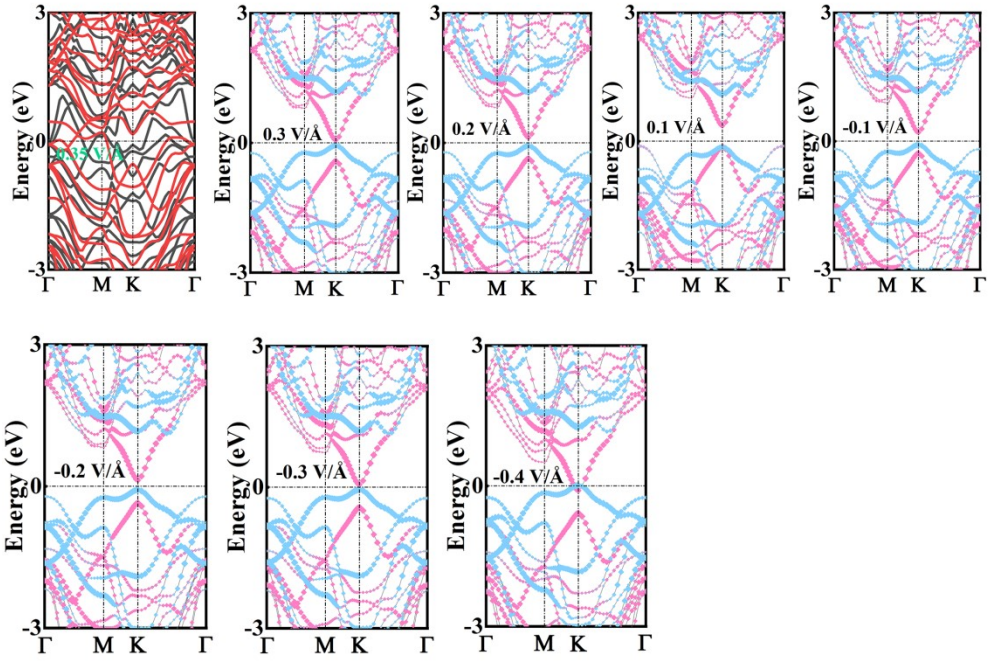

Fig. S10. The projected band structures of the $WSi_2P_4/MoTe_2$ vdWHs under different external electric fields